Peptides 55 (2014) 92–97

Contents lists available at ScienceDirect

Peptides

journal homepage: www.elsevier.com/locate/peptides

Native and recombinant Pg-AMP1 show different antibacterial activity spectrum but similar folding behavior

William F. Porto[a], Diego O. Nolasco[a,b], Octavio L. Franco[a,*]

[a] Centro de Análises Proteômicas e Bioquímicas, Pós-Graduação em Ciências Genômicas e Biotecnologia, Universidade Católica de Brasília, Brasília, DF, Brazil
[b] Curso de Física, Universidade Católica de Brasília, Brasília, DF, Brazil

ARTICLE INFO

Article history:
Received 13 January 2014
Received in revised form 18 February 2014
Accepted 18 February 2014
Available online 26 February 2014

Keywords:
Plant glycine-rich proteins
Antimicrobial peptides
Ab initio molecular modelling
Molecular dynamics
Solvated potential energy

ABSTRACT

Glycine-rich proteins (GRPs) derived from plants compose a family of proteins and peptides that share a glycine repeat domain and they can perform diverse functions. Two structural conformations have been proposed for GRPs: glycine loops arranged as a Velcro and an anti-parallel β-sheet with several β-strands. The antimicrobial peptide Pg-AMP1 is the only plant GRP with antibacterial activity reported so far and its structure remains unclear. Recently, its recombinant expression was reported, where the recombinant peptide had an additional methionine residue at the N-terminal and a histidine tag at the C-terminal (His_6-tag). These changes seem to change the peptide's activity, generating a broader spectrum of antibacterial activity. In this report, through *ab initio* molecular modelling and molecular dynamics, it was observed that both native and recombinant peptide structures were composed of an N-terminal α-helix and a dynamic loop that represents two-thirds of the protein. In contrast to previous reports, it was observed that there is a tendency to adopt a globular fold instead of an extended one, which could be in both, glycine loops or anti-parallel β-sheet conformation. The recombinant peptide showed a slightly higher solvated potential energy compared to the native form, which could be related to the His_6-tag exposition. In fact, the His_6-tag could be mainly responsible for the broader spectrum of activity, but it does not seem to cause great structural changes. However, novel studies are needed for a better characterization of its pharmacological properties so that in the future novel drugs may be produced based on this peptide.

1. Introduction

The plant glycine-rich proteins (GRPs) compose a family of proteins and peptides that share a glycine repeat domain [22]. This domain provides high flexibility for these molecules and for this reason the GRPs seem to be good candidates for function conjugation with other proteins and multiple macromolecules [22].

Structurally, two conformations have been proposed for GRPs. The first is composed of glycine loops arranged as a Velcro, through the packing of the interspersed non-glycine residues. In this situation, the glycine loops would seem to be responsible for protein-protein interactions, generating quaternary structures [22]. The second proposed conformation is an anti-parallel β-sheet with several β-strands, where the side chains of bulky residues would be projected on the same side, generating a large hydrophobic surface, available for interactions with other hydrophobic molecules, such as the cell wall or membrane [22].

Since the late 80's, a large number of GRPs have been described with diverse functions that could be related to distinctive motifs (*e.g.* RNA binding motifs, RNA recognition motifs, cold shock domains and CCHC zinc-fingers). The GRPs with low glycine content (about 20%) present the more diverse repertoire of distinctive motifs, including amphipathic α-helices, oleosin domains, and histidine-rich, proline-rich and threonine rich domains [22].

In 2008, Pelegrini et al. [20] isolated an antibacterial GRP with low glycine content from guava (*Psidium guajava*) seeds, the *P. guajava* antimicrobial peptide 1 (Pg-AMP1). Pg-AMP1 was mainly active against Gram-negative bacteria, including *Klebsiella pneumoniae* and *Escherichia coli* (Table 1). Recently, Tavares et al. [26] have reported the heterologous expression of Pg-AMP1, with two modifications: the addition of a methionine residue and a histidine tag (His_6-tag) at the N- and C-terminals, respectively. Interestingly, recombinant Pg-AMP1 showed different activities in relation to the original peptide, being able to inhibit the development of Gram-negative and Gram-positive bacteria (Table 1). The novel activities

* Corresponding author. Tel.: +55 61 34487167/34487220; fax: +55 61 33474797.
E-mail address: ocfranco@gmail.com (O.L. Franco).
URL: http://www.capb.com.br (O.L. Franco).

http://dx.doi.org/10.1016/j.peptides.2014.02.010
0196-9781/

Table 1
Antimicrobial activity of native and recombinant Pg-AMP1. MIC corresponds to minimum inhibitory concentration.

Bacteria	Gram stain	MIC ($\mu g\,mL^{-1}$)	
		Native Pg-AMP1	Recombinant Pg-AMP1
Staphilococcus aureus[a]	Positive	NO	50
Staphilococcus epidermides[b]	Positive	NT	100
Klebsiella pneumoniae[c]	Negative	32	100
Pseudomonas aeruginosa[d]	Negative	NT	100
Escherichia coli[e]	Negative	72	100

NO, not observed. NT, not tested.
[a] ATCC 3359-1 and 2921-3 for the recombinant peptide; not described for the native one.
[b] ATCC 1122-8.
[c] ATCC 13883 for the native Pg-AMP1 and 13866 for the recombinant one.
[d] ATCC 27853.
[e] ATCC 8739 for the native Pg-AMP1 and ATCC 11229 and 35218 for the recombinant one.

seem to be related to increase in positive net charge due to the His_6-tag addition. However, three-dimensional structural predictions indicated that the His_6-tag could not cause structural changes in the Pg-AMP1. Native and recombinant Pg-AMP1 were predicted to have an N-terminal α-helix and a large random coil comprising the final two-thirds of the peptide. This prediction was in contrast with the first report from Pelegrini et al. [20], which posited that Pg-AMP1 has two terminal α-helices connected by the glycine-rich portion.

In this study, a set of short molecular dynamics simulations of the native and the recombinant Pg-AMP1 was performed in a water environment. In this context, we verified which conformation (glycine loops or β-sheet) is predominantly assumed for both peptides after 100 ns of simulation and whether there are differences in the solvated potential energy of both peptides.

2. Material and methods

2.1. Molecular modelling

Molecular modelling was performed according to Tavares et al. [26]. The molecular models were generated by the *ab initio* molecular modelling server QUARK [28] in order to create an initial structure. Then, 100 structures were generated by the Modeller's loop-refinement sub routine [5] using the *ab initio* structure as template. The region to be refined was selected according to the information given by the Protein DisOrder prediction System (PrDOS) [10]. The final model was selected according to the discrete optimized protein energy (DOPE) scores. This score assesses the energy of the model and indicates the most probable structures. The final model was evaluated through Verify 3D [13], ProSA II [27] and PROCHECK [11]. PROCHECK checks the stereo chemical quality of a protein structure, through the Ramachandran plot, where reliable models are expected to have more than 90% of the amino acid residues in the most favored and allowed regions, while ProSA II indicates the fold quality; in addition, Verify 3D analyses the compatibility of an atomic model (3D) with its own amino acid sequence (1D). Structure visualization was done in PyMOL (The PyMOL Molecular Graphics System, Version 1.4.1, Schrödinger, LLC).

2.2. Molecular dynamics

The molecular dynamics simulations (MD) were carried out in a water environment, using the Single Point Charge water model [2]. The analyses were performed by using the GROMOS96 43A1 force field and the computational package GROMACS 4 [8]. The dynamics used molecular models generated by Modeller as the initial structures. The initial structures were immersed in water molecules in a cubic box. The minimum distance between the peptide and the edge of the box was set to 0.7 nm. Chlorine ions were added in order to neutralize the system charge. The geometry of water molecules was constrained by using the SETTLE algorithm [17]. All atom bond lengths were linked by using the LINCS algorithm [7]. Electrostatic corrections were made by Particle Mesh Ewald algorithm [4], with a cut-off radius of 1.4 nm in order to minimize the computational time. The same cut-off radius was also used for van der Waals interactions. The list of neighbors of each atom was updated every 10 simulation steps of 2 fs. The system underwent an energy minimization using 50,000 steps of the steepest descent algorithm. After that, the system temperature was normalized to 300 K for 100 ps, using the velocity rescaling thermostat (NVT ensemble). Furthermore, the system pressure was normalized to 1 bar for 100 ps, using the Parrinello–Rahman barostat (NPT ensemble). The systems with minimized energy, balanced temperature and pressure were simulated for 100 ns by using the leap-frog algorithm. The trajectories were evaluated through RMSD and Radius of Gyration. Each simulation was repeated three times.

2.3. Solvated potential energy calculation

The peptide structures were taken every 10 s of molecular dynamics simulation and their solvated potential energy was calculated through the Adaptive Poisson–Boltzmann Solver (APBS) [1]. For visualization, surface potentials were set to $\pm 5\,kTe^{-1}$ (133.56 mV).

2.4. Statistical analysis

A one-sided Wilcoxon–Mann–Whitney non-parametric test was applied for verifying whether the solvated potential energy of recombinant Pg-AMP1 is higher than that of the native form, with a critical value of 0.05, taking into account the structures at 100 ns of simulation. The statistical analyses were done through the R package for statistical computing (http://www.r-project.org).

3. Results

3.1. Native Pg-AMP1

For molecular modelling, an *ab initio* technique was used for three-dimensional structure prediction. Initially, a preliminary structure was constructed by QUARK and then refined by Modeller, generating 100 refined models. The best model showed a DOPE score of −2723.638672. On Verify 3D, the best model showed a minimum and a maximum 1D–3D average score of 0.22 and 0.88, respectively. In the Ramachandran plot, the final model showed that 72.2% of the residues are in favored regions, 19.4% are in additional allowed regions and 5.6% are in generously allowed regions. The model has a G-Factor of −0.75 and the *Z*-Score on ProSA was −2.81, indicating a valid molecular model. The model was composed of an α-helix (residues Pro^4 to Arg^{16}) and a large coil which comprises two-thirds of the structure (Fig. 1A). This coil was predicted to be in disorder by PrDOS, as previously described by Tavares et al. [26].

Because of the dynamic character of native Pg-AMP1 structure, in the molecular dynamics simulations, the root mean square deviation (RMSD) values comparing the initial and the final structures were above 5 Å (Fig. 1B), indicating a clear structural modification (Fig. 1A). In fact, the structure underwent compression due to the folding process of the random coil, which was clearly indicated by the radius of gyration of 1.079 ± 0.086 nm (Fig. 2A), and was mainly responsible for the structural modification in the three simulations.

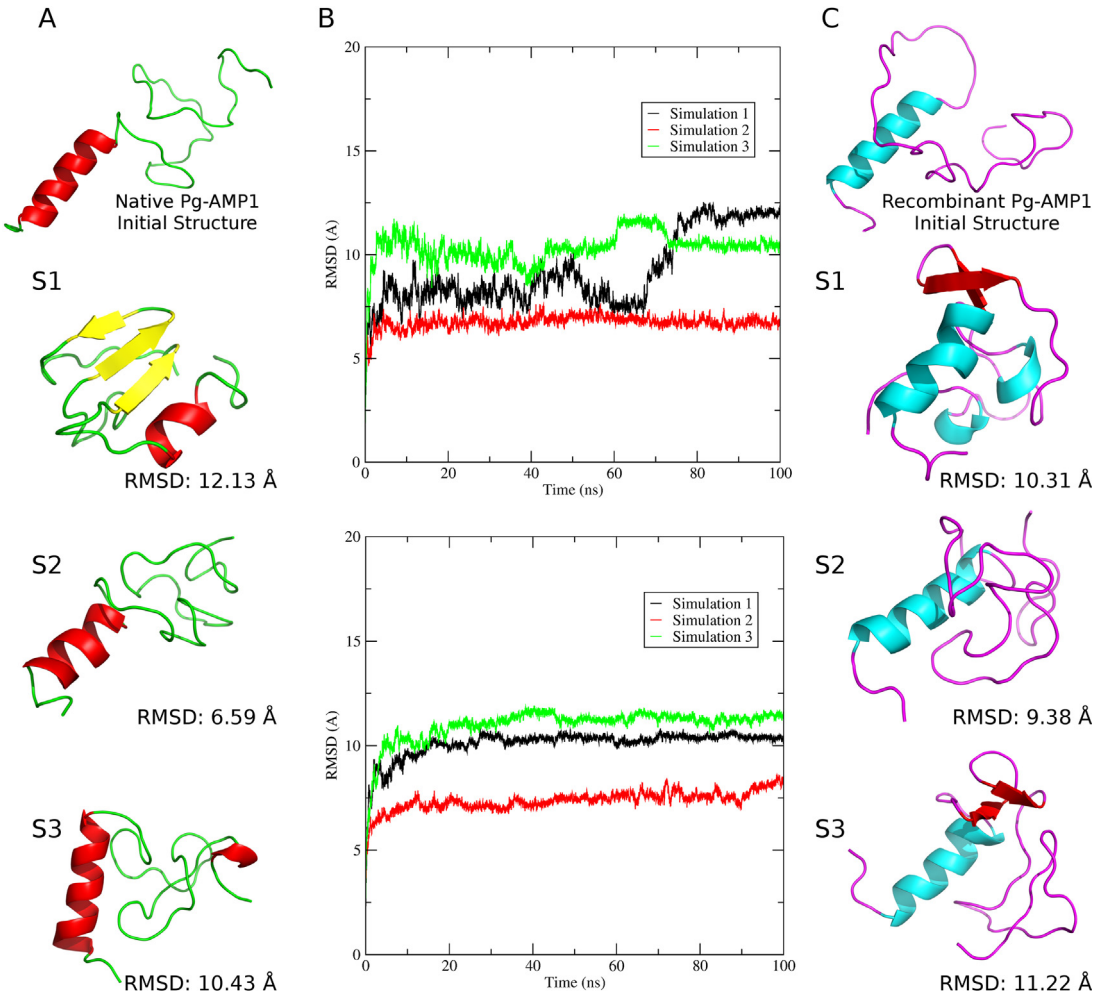

Fig. 1. Molecular dynamics simulations of native and recombinant Pg-AMP1. (A) Native Pg-AMP1 structures: initial structure (top) and final structures at 100 ns in three simulations (S1, S2 and S3). (B) RMSD evolution during the simulations for native (top) and recombinant forms (bottom): simulation 1 (black lines), 2 (red lines) and 3 (green lines). (C) Recombinant Pg-AMP1 structures: initial structure (top) and final structures at 100 ns in three simulations (S1, S2 and S3). (For interpretation of the references to color in this figure legend, the reader is referred to the web version of the article.)

The three simulations of native Pg-AMP1 did not converge to a consensus structure (Fig. 1A). In fact, the only structural element conserved among the three simulations was the N-terminal α-helix. However, the α-helix extension varied from one simulation to another, varying from six (Met^{8} to Gln^{13}), to eleven (Ser^{6} to Arg^{16}) or fourteen residues (Pro^{4} to Tyr^{17}). The remaining structure was variable: in the first simulation, it assumed an anti-parallel β-sheet; while in the other two, it assumed a random structure (Fig. 1). In addition, the electrostatic surface indicated that the native Pg-AMP1 is an amphipathic molecule with large cationic patches (Fig. 3), but the solvated potential energy decreases as the peptide folds, starting from 1814.2 kJ/mol from the initial structure to, on average, 1627.6 ± 190 kJ/mol from the structure at 100 ns of simulation (Fig. 2). Therefore, the native Pg-AMP1 structure is composed of an N-terminal α-helix and a random segment, and its solvated potential energy decreases as the peptide folds.

3.2. Recombinant Pg-AMP1

The same modeling procedure was applied to recombinant Pg-AMP1, generating a final model with a DOPE score of −3429.208008. The recombinant Pg-AMP1 model showed a minimum and a maximum 1D–3D average score of 0.2 and 0.74, respectively, on Verify 3D. In the Ramachandran plot, the final model showed that 65.1% of the residues are in favored regions, 25.6% are in additional allowed regions and 9.3% are in generously allowed regions. The model has a G-Factor of −0.78 and the *Z*-Score on ProSA was −2.67, indicating a valid molecular model with similar quality to the native Pg-AMP1 model. As observed for the native peptide, the recombinant Pg-AMP1 model was composed of an α-helix (residues Pro^{4} to Tyr^{18}) and a large coil, also comprising two-thirds of the structure (Fig. 1C). This coil was also predicted to be in disorder by PrDOS, as previously described by Tavares et al. [26].

The recombinant Pg-AMP1 structure showed similar behavior to the native peptide, presenting a very dynamic structure, with RMSD values above 7 Å when comparing the initial and final structures from molecular dynamics (Fig. 1B). As observed for the native Pg-AMP1, the recombinant peptide did not converge to a consensus structure during the three simulations. However, the N-terminal α-helix was maintained in the three simulations (Fig. 1C), as well as the His_6-tag exposure (Fig. 4). In two simulations, a short β-hairpin could be observed. In addition, the recombinant peptide also underwent a structure compression during the simulation (Fig. 2), with a final radius of gyration of 1.076 ± 0.057 nm. Moreover, the solvated potential energy also decreases as the peptide folds, moving from 1985.1 kJ/mol from the initial structure to 1728.7 ± 123 kJ/mol, on average, from the structure at 100 ns of simulation (Fig. 3).

Despite this similar behavior, the major difference between the native and the recombinant Pg-AMP1 was in electrostatic

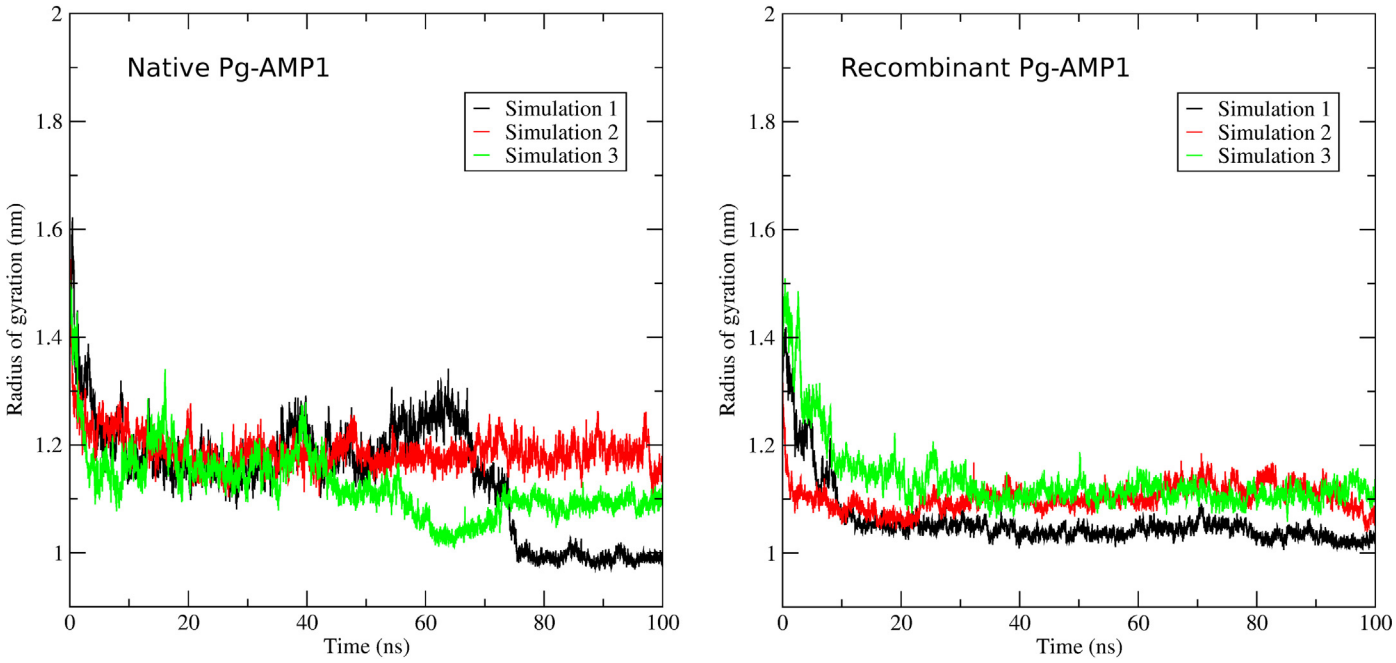

Fig. 2. The radius of gyration evolution during the simulations for native (left) and recombinant forms (right): simulation 1 (black lines), 2 (red lines) and 3 (green lines). (For interpretation of the references to color in this figure legend, the reader is referred to the web version of the article.)

potential. Even with a similar amphipathic electrostatic surface, with large cationic patches (Fig. 2), the solvated potential energy is somewhat higher than the native one (Fig. 2), but no statistical difference was observed, with a *P*-value of 0.5 in the one-sided Wilcoxon–Mann–Whitney non-parametric test.

4. Discussion

To date, over 200 antimicrobial peptides (AMPs) have been reported from plants [3]. These compounds have been recognized as playing a pivotal role in plant defense. Therefore, these compounds have seen their structure–activity relationship widely investigated [3,19].

The majority of plant AMPs are cysteine-rich [3,19,24], with few examples of plant disulfide-free AMPs [14,15,20,23,26]. Among the disulfide-free AMPs, Pg-AMP1 is the only plant GRP reported to be active against bacteria so far, although GRPs from animals may also be active against bacteria [9,12].

Recently, the heterologous expression of Pg-AMP1 was reported, with two modifications in the original sequence, the addition of a methionine residue at the N-terminal and a His_6-tag at the C-terminal. These sequence modifications led to an interesting change in the antibacterial activity spectrum: while recombinant Pg-AMP1 became active against Gram-positive bacteria, its potency against Gram-negative bacteria was reduced in comparison to the native peptide [26].

In order to investigate what kind of structural variations the modifications for heterologous expression could lead to and also to verify what kind of conformations these peptides can adopt, *ab initio* molecular modelling followed by molecular dynamics was applied, which are the same methods previously applied to studying other plant AMPs structures [16,21].

Molecular modelling indicated that the both forms of Pg-AMP1 adopt a structure composed of an N-terminal α-helix followed by the unstructured portion, which includes the glycine-rich portion, in an extended conformation, as described by Tavares et al. [26]. These structures are in agreement with other GRPs with similar glycine content, which have α-helixes in their structures [6,18].

Although the initial structures adopt an extended conformation, during the simulations the structures underwent compression as indicated by the average radius of gyration of 1.079 ± 0.086 nm and 1.076 ± 0.057 nm for native and recombinant forms, respectively (Fig. 2). This compression is also related to the high RMSD values observed, clearly indicating a fold change during the simulations (Fig. 1).

Since two-thirds of the Pg-AMP1 structure has no defined structure, this dynamic behavior was expected, with the N-terminal α-helix as the only conserved structural element, which is in disagreement with the first structure prediction of Pg-AMP1, a dimer structure with two α-helixes [19]. However, due to the random character of Pg-AMP1, the first proposed structure could also occur. Here, the monomer structures were used instead of the dimer, since the dimer form occurs in small quantities [20,26].

Overall, it has been proposed that GRPs should adopt a β-sheet structure or a structure composed of glycine loops. What could be observed in the simulations was the possibility of forming both structures in independent runs (Fig. 1). However, glycine loops are predominant in the native Pg-AMP1 structure, while in the recombinant peptide there is a predominance of a hybrid structure with a short β-hairpin followed by glycine loops (Fig. 1). Perhaps, in water environment the two structures coexist for both forms of Pg-AMP1.

There are two major differences between the spectrum of antimicrobial activity of native and recombinant Pg-AMP1, (i) the MIC against Gram-negative bacteria is higher for the native peptide and (ii) the native peptide is unable to inhibit the growth of Gram-positive bacteria (Table 1). The reduction in activity against Gram-negative bacteria seems to be related a technical reason, since the recombinant peptide was dissolved in saline solution [26], while the native one was dissolved in Milli-Q water [20] and it is known that higher salt concentrations could decrease the antimicrobial activity [25]. The second difference could be related to the modifications for heterologous expression. Although the mechanism of action of Pg-AMP1 is still unclear; it seems to be changed by these modifications, since the recombinant peptide has a broad-spectrum of antimicrobial activity when compared to the native one. The N-terminal methionine is capable of increase the

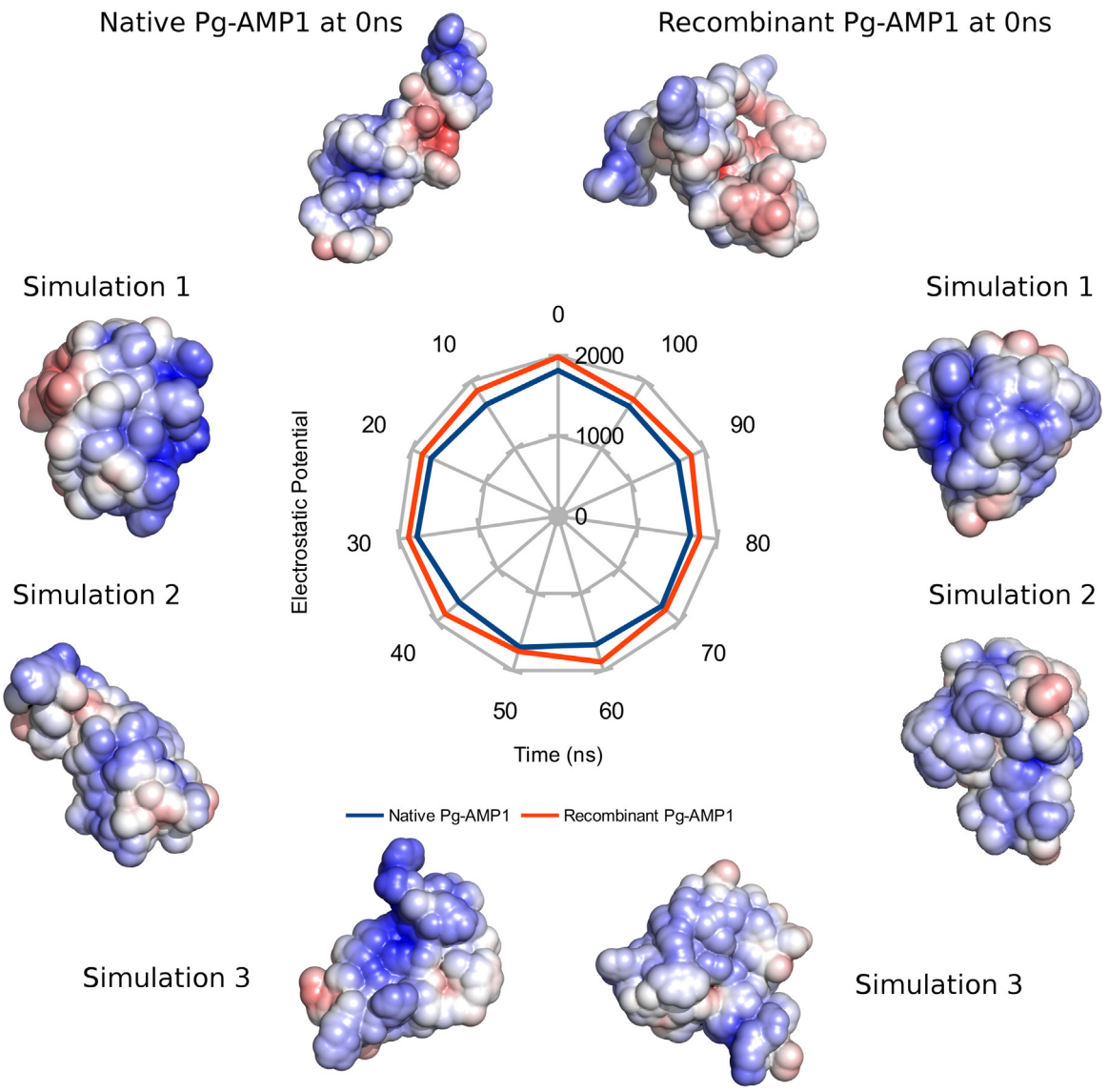

Fig. 3. Electrostatic surface and solvated potential energy of native and recombinant Pg-AMP1. The native form is represented by left surfaces, while the recombinant one by right surfaces, with the initial surface at the top. The cationic patches are highlighted. The radar graph at the center represents the evolution of average solvated potential energy during the simulations: blue for the native peptide and orange for the recombinant one.

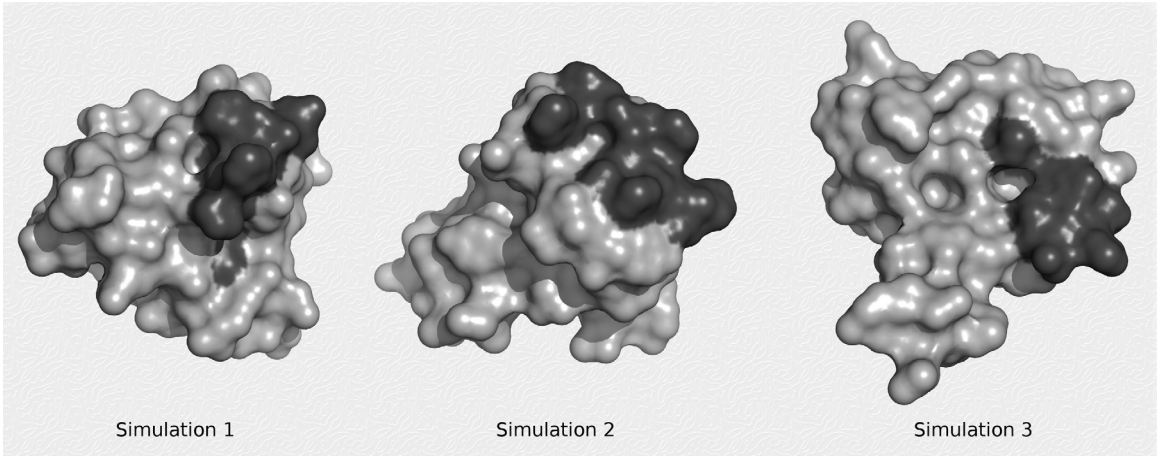

Fig. 4. Exposition of His_6-tag on the surface of recombinant Pg-AMP1 final structures after 100 ns of simulation. The His_6-tag is displayed in dark gray.

peptide hydrophobicity. Nevertheless, the cationic properties of His6-tag hinder such amino acid residue, suppressing the methionine hydrophobicity. Therefore the N-terminal methionine acts only as the start codon for heterologous expression. Tavares et al. [26] suggested that His_6-tag increased Pg-AMP1 affinity to bacterial membrane since the His_6-tag increased the net charge by +6, leading to a more cationic peptide. However, depending on the peptide fold, this assumption may not be true. In an extended conformation all charges could be exposed, while in a compact fold, some charged residues could be buried.

To verify this issue, the solvated potential energy was calculated at every 10 ns of simulation, and this potential decreased with the peptide folds in both cases, indicating that some charged groups could be buried for both peptide forms (Fig. 3). Despite this solvated potential energy reduction, the structures are still amphipathic with a large cationic patch. Overall, recombinant Pg-AMP1 has a higher solvated potential energy than the native one, showing 1728.7 ± 123 and 1627.6 ± 190 kJ/mol, respectively, at the end of simulations (Fig. 3). Although there is no statistical difference between these energies (P-value of 0.5), this difference should be biologically significant, since the recombinant peptide is more attracted to the bacteria, which could result in a broader spectrum of antibacterial activity.

5. Conclusion

Both forms of Pg-AMP1 have a very dynamic structure. The molecular dynamics simulations showed this character once more. However, the simulations indicated that the peptide does not adopt an extended fold in either form, as previously posited based only on *ab initio* molecular modelling [26]. It could be observed that there is a structure compression during the simulations, leading to a more globular fold, and the structure could adopt both glycine loops and β-sheet conformations. In fact, the His_6-tag could be mainly responsible for the broader spectrum of activity; however, it does not seem to cause great structural changes. The His_6-tag led to a potential increase in solvated energy in the recombinant form, since it became exposed during the simulations. Indeed, the Pg-AMP1 is the only plant GRP reported to be active against bacteria so far and it role in guava biology is still unclear, despite its antimicrobial function. In addition, new studies are needed for a better characterization of its structural and pharmacological properties, such as circular dichroism or nuclear magnetic resonance. In this context novel and potent drugs may be designed and produced based on this peptide scaffold in a near future.

Acknowledgments

The authors are grateful to the Center for Scientific Computing (NCC/GridUNESP) of São Paulo State University (UNESP), the Conselho Nacional de Desenvolvimento Científico e Tecnológico (CNPq), Coordenação de Aperfeiçoamento de Pessoal de Nível Superior (CAPES), Fundação de Amparo a Pesquisa do Distrito Federal (FAPDF) and Universidade Católica de Brasília (UCB) for support.

References

[1] Baker NA, Sept D, Joseph S, Holst MJ, McCammon JA. Electrostatics of nanosystems: application to microtubules and the ribosome. Proc Natl Acad Sci U S A 2001;98(18):10037–41.
[2] Berendsen HJC, Postma JPM, van Gunsteren WF, Hermans J. Interaction models for water in relation to protein hydration. In: Pullman B, editor. Intermolecular force. Dordrecht: Reidel; 1981. p. 331–42, http://dx.doi.org/10.1007/978-94-015-7658-1_21.
[3] Cândido ES, Porto WF, Amaro DS, Viana JC, Dias SC, Franco OL. Structural and functional insights into plant bactericidal peptides. In: Méndez-Vilas A, editor. Science against microbial pathogens: communicating current research and technological advances. Formatex; 2011. p. 951–60.
[4] Darden T, York D, Pedersen L. Particle mesh Ewald: an $n\log(n)$ method for Ewald sums in large systems. J Chem Phys 1993;98(12):10089–92, http://dx.doi.org/10.1063/1.464397.
[5] Eswar N, Webb B, Marti-Renom MA, Madhusudhan M, Eramian D, Shen MY, et al. Comparative protein structure modeling using MODELLER. Curr Protoc Protein Sci 2007, http://dx.doi.org/10.1002/0471140864.ps0209s50.
[6] Godoy JA, Pardo JM, Pintor-Toro JA. A tomato cDNA inducible by salt stress and abscisic acid: nucleotide sequence and expression pattern. Plant Mol Biol 1990;15(5):695–705.
[7] Hess B, Bekker H, Berendsen HJC, Fraaije JGEM. LINCS. A linear constraint solver for molecular simulations. J Comp Chem 1997;18(12):1463–72, http://dx.doi.org/10.1002/(SICI)1096-987X(199709)18:12<1463::AID-JCC4>3.0.CO;2-H.
[8] Hess B, Kutzner C, van der Spoel D, Lindahl E. GROMACS 4: algorithms for highly efficient, load-balanced, and scalable molecular simulation. J Chem Theory Comput 2008;4(3):435–47.
[9] Imjongjira KC, Amparyup P, Tassanakajon A. Two novel antimicrobial peptides, arasin-like spand GRPSp, from the mud crab *Scylla paramamosain*, exhibit the activity against some crustacean pathogenic bacteria. Fish Shellfish Immunol 2011;30:706–12.
[10] Ishida T, Kinoshita K. PrDOS. Prediction of disordered protein regions from amino acid sequence. Nucl Acids Res 2007;35:1–5.
[11] Laskowski RA, MacArthur MW, Moss DS, Thornton JM. PROCHECK: a program to check the stereochemical quality of protein structures. J Appl Cryst 1993;26(2):283–91, http://dx.doi.org/10.1107/S0021889892009944.
[12] Lu J, Chen ZW. Isolation, characterization and anti-cancer activity of SK84, a novel glycine-rich antimicrobial peptide from *Drosophila virilis*. Peptides 2010;31:44–50.
[13] Lüthy R, Bowie JU, Eisenberg D. Assessment of protein models with three-dimensional profiles. Nature 1992;356(6364):83–5.
[14] Mandal SM, Dey S, Mandal M, Sarkar S, Maria-Neto S, Franco OL. Identification and structural insights of three novel antimicrobial peptides isolated from green coconut water. Peptides 2009;30(4):633–73.
[15] Mandal SM, Migliolo L, Das S, Mandal M, Franco OL, Hazra TK. Identification and characterization of a bactericidal and proapoptotic peptide from *Cycas revoluta* seeds with DNA binding properties. J Cell Biochem 2012;113:184–93.
[16] Mandal SM, Porto WF, Dey P, Maiti MK, Ghosh AK, Franco OL. The attack of the phytopathogens and the trumpet solo: Identification of a novel plant antifungal peptide with distinct fold and disulfide bond pattern. Biochimie 2013;95(10):1939–48.
[17] Miyamoto S, Kollman PA. SETTLE. An analytical version of the SHAKE and RATTLE algorithm for rigid water models. J Comp Chem 1992;13(8):2134–44, http://dx.doi.org/10.1002/jcc.540130805.
[18] Mundy J, Chua NH. Abscisic acid and water-stress induce the expression of a novel rice gene. EMBO J 1988;7(8):2279–86.
[19] Padovan L, Scocchi M, Tossi A. Structural aspects of plant antimicrobial peptides. Curr Protein Pept Sci 2010;11(3):210–9.
[20] Pelegrini PB, Murad AM, Silva LP, Dos Santos RC, Costa FT, Tagliari PD, et al. Identification of a novel storage glycine-rich peptide from guava (*Psidium guajava*) seeds with activity against Gram-negative bacteria. Peptides 2006;29(8):1271–9.
[21] Porto WF, Franco OL. Theoretical structural insights into the snakin/GASA family. Peptides 2013;44:163–7.
[22] Sachetto-Martins G, Franco LO, de Oliveira DE. Plant glycine-rich proteins: a family or just proteins with a common motif. Biochim Biophys Acta 2000;1492:1–14.
[23] Silva ON, Porto WF, Migliolo L, Mandal SM, Gomes DG, Holanda HH, et al. Cn-AMP-1: a new promiscuous peptide with potential for microbial infections treatment. Biopolymers 2012;98(4):322–31.
[24] Silverstein KAT, Moskal WA, Wu HC, Underwood BA, Graham MA, Town CD, et al. Small cysteine-rich peptides resembling antimicrobial peptides have been under-predicted in plants. Plant J 2007;51(2):262–80.
[25] Tam JP, Lu YA, Yang JL, Chiu KW. An unusual structural motif of antimicrobial peptides containing end-to-end macrocycle and cystine-knot disulfides. Proc Natl Acad Sci U S A 1999;96(16):8913–8.
[26] Tavares LS, Rettore JV, Freitas RM, Porto WF, Duque AP, Singulani de L, et al. Antimicrobial activity of recombinant Pg-AMP1, a glycine-rich peptide from guava seeds. Peptides 2012;37(2):294–300.
[27] Wiederstein M, Sippl MJ. ProSA-web: interactive web service for the recognition of errors in three-dimensional structures of proteins. Nucl Acids Res 2007;35:W407–10.
[28] Xu D, Zhang Y. Ab initio protein structure assembly using continuous structure fragments and optimized knowledge-based force field. Proteins 2012;80:1715–35, http://dx.doi.org/10.1002/prot.24065.